International Journal of Solids and Structures 49 (2012) 2590–2603

Contents lists available at SciVerse ScienceDirect

International Journal of Solids and Structures

journal homepage: www.elsevier.com/locate/ijsolstr

Effective thermoelastic properties of composites with periodicity in cylindrical coordinates

George Chatzigeorgiou [a,*], Yalchin Efendiev [b], Nicolas Charalambakis [a], Dimitris C. Lagoudas [c]

[a] Institute of Mechanics of Materials, Dept. of Civil Engineering, Aristotle University of Thessaloniki, Thessaloniki 54124, Greece
[b] Dept. of Mathematics, Texas A&M University, College Station, TX 77843, USA
[c] Dept. of Aerospace Engineering, Texas A&M University, College Station, TX 77843, USA

ARTICLE INFO

Article history:
Received 15 June 2011
Received in revised form 29 April 2012
Available online 15 June 2012

Keywords:
Asymptotic expansion homogenization method
Micromechanics
Thermomechanical response
Microscale response

ABSTRACT

The aim of this work is to study composites that present cylindrical periodicity in the microstructure. The effective thermomechanical properties of these composites are identified using a modified version of the asymptotic expansion homogenization method, which accounts for unit cells with shell shape. The microscale response is also shown. Several numerical examples demonstrate the use of the proposed approach, which is validated by other micromechanics methods.

1. Introduction

The rapid technological development that has been achieved the recent years has led to the appearance of a plenty of new composite materials with multifunctional behavior. Nowadays there is a large variety of composite materials, such as the multilayered, the fiber and the particulate composites, which can be used in many structural applications. The, relatively new, nanocomposites based on carbon nanotubes (Iijima, 1991) allow the construction of strong and light structures and they are already used in industrial applications. The newly developed functionally graded materials provide excellent thermomechanical properties (Miyamoto et al., 1999).

The major criterion for the selection and design of a composite material in engineering structures is the good mechanical and thermal performance. The identification of the composite material behavior though is a difficult task and in many cases approximate methods are used (Pindera et al., 2009). The position and the geometry of the constituent materials, the void nucleation during the construction of the composite material and the appearance of weak interphases between two different materials due to bad coherence are only a few of the problems for determining the thermomechanical behavior of the actual composite structure.

The basic theoretical tools for the estimation of the thermomechanical response of composite materials are the micromechanics and the homogenization methods (Bensoussan et al., 1978; Bakhvalov and Panasenko, 1989; Kalamkarov and Kolpakov, 1997; Qu and Cherkaoui, 2006). The aim of these methods is to determine the effective behavior of the composite material using the properties, the volume fractions and the geometrical structure of the constituent materials. Emerging theories provide efficient computational approaches of functionally graded materials (Cavalcante et al., 2007).

Very recently, an increased research interest for materials and structures with cylindrical geometry has appeared (Horgan and Chan, 1999a,b; Chen et al., 2000; Tarn and Wang, 2001; Tarn, 2002; Ruhi et al., 2005; Kordkheili et al., 2007; Chatzigeorgiou et al., 2008; Chatzigeorgiou et al., 2009; Tsukrov and Drach, 2010; Nie and Batra 2010a–c; Gélébart, 2011; Cavalcante et al., 2011). Material systems that present non-homogeneous structure with cylindrical geometry can be found in engineering applications (composite shells, composite materials with carbon nanotubes, carbon fibers, tubular hybrid composites), biomedical applications (study of bones and tissues) and natural systems (bamboo, tree trunk). The determination of the overall behavior of such structures require the use of appropriate homogenization tools.

The subject of this paper is the homogenization of structures with periodic shell (e.g. cylindrical) structure and the computation of their effective thermomechanical response. Methodology for obtaining the effective mechanical properties for these structures was introduced in Chatzigeorgiou et al. (2011), using a modified version of the asymptotic expansion homogenization method (AEH) for shell type periodic unit cells. In this work we extend the methodology to include also effective thermal properties, as

* Corresponding author.
E-mail address: ghatzige@civ-engin.com (G. Chatzigeorgiou).

0020-7683/$ - see front matter © 2012 Elsevier Ltd. All rights reserved.
http://dx.doi.org/10.1016/j.ijsolstr.2012.05.023

well as to present the microscale thermomechanical response of composite structures with cylindrical periodicity. Moreover, emphasis is given on some engineering applications of special interest, such as FRP-wrapped concrete cylindrical columns, and the interphase of "fuzzy fiber" composites. The interesting characteristic of the material systems under investigation is that their structures are produced by the repetition of a unit cell with macrovariable-dependent elementary volume. This characteristic is taken into account in the present work. We note that in this paper a complete set of homogenized coefficients is given and microstructural response is identified. Local stress field disturbances due to materials architecture have an impact on the interfacial strength (Lekhnitskii, 1981).

The structure of the paper is the following: Section 2 presents the general framework and the basic thermomechanical equations that describe the behavior of the composite's material constituents. Section 3 describes the AEH method for microscale structure with cylindrical periodicity. Several numerical examples motivated by engineering applications are presented in Section 4. The first example refers to the homogenization of multilayered tubes. In the second and third example we determine the effective properties of unidirectional and two-directional fiber reinforced polymers-wrapped concrete columns. In the fourth example we compute the effective thermomechanical properties of the interphase in "fuzzy fiber" composites. The last Section includes the major conclusions of this work.

2. Materials with periodic shell structure

This work focuses on composite tubes with cylindrical periodicity in the microstructure. The schematic of Fig. 1 represents such a composite. The representative element in this structure has macrovariable-dependent elementary volume, in the sense that its volume increases as we move from the inner to the outer surface of the tube.

Each constituent of the composite is assumed to exhibit linear thermoelastic response. Due to the cylindrical geometry of the composite, it is more convenient to represent the equations that characterize the thermomechanical behavior of the constituents in cylindrical coordinate system. For each material the strains $\boldsymbol{\varepsilon}$ are given in terms of the displacements $\boldsymbol{u}$

$$\begin{aligned}
&\varepsilon_{rr}=\frac{\partial u_r}{\partial r},\quad \varepsilon_{\theta\theta}=\frac{1}{r}\left(\frac{\partial u_\theta}{\partial\theta}+u_r\right),\\
&\varepsilon_{zz}=\frac{\partial u_z}{\partial z},\quad \varepsilon_{z\theta}=\frac{1}{2}\left(\frac{\partial u_\theta}{\partial z}+\frac{1}{r}\frac{\partial u_z}{\partial\theta}\right),\\
&\varepsilon_{rz}=\frac{1}{2}\left(\frac{\partial u_z}{\partial r}+\frac{\partial u_r}{\partial z}\right),\quad \varepsilon_{r\theta}=\frac{1}{2}\left(\frac{1}{r}\frac{\partial u_r}{\partial\theta}+\frac{\partial u_\theta}{\partial r}-\frac{u_\theta}{r}\right).
\end{aligned}\tag{1}$$

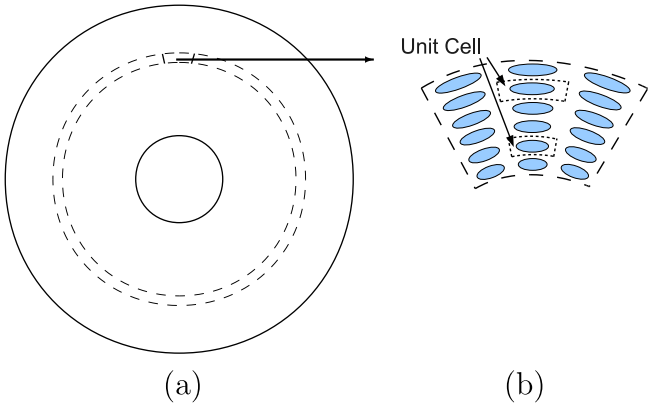

Fig. 1. Composite with periodic shell structure and a zoomed area which shows the unit cells.

The stress–strain ($\boldsymbol{\sigma}$–$\boldsymbol{\varepsilon}$) thermoelastic constitutive laws, using the Voigt notation,[1] are given by

$$\boldsymbol{\sigma}=\boldsymbol{C}\left[\boldsymbol{\varepsilon}-\boldsymbol{\alpha}(\vartheta-\vartheta_{ref})\right],\tag{2}$$

where

$$\boldsymbol{\sigma}=\begin{bmatrix}\sigma_{rr}\\ \sigma_{\theta\theta}\\ \sigma_{zz}\\ \sigma_{z\theta}\\ \sigma_{rz}\\ \sigma_{r\theta}\end{bmatrix},\quad \boldsymbol{C}=\begin{bmatrix}C_{rrrr} & C_{rr\theta\theta} & C_{rrzz} & C_{rr\theta z} & C_{rrrz} & C_{rrr\theta}\\ C_{rr\theta\theta} & C_{\theta\theta\theta\theta} & C_{\theta\theta zz} & C_{\theta\theta\theta z} & C_{\theta\theta rz} & C_{\theta\theta r\theta}\\ C_{rrzz} & C_{\theta\theta zz} & C_{zzzz} & C_{zz\theta z} & C_{zzrz} & C_{zzr\theta}\\ C_{rr\theta z} & C_{\theta\theta\theta z} & C_{zz\theta z} & C_{\theta z\theta z} & C_{\theta zrz} & C_{\theta zr\theta}\\ C_{rrrz} & C_{\theta\theta rz} & C_{zzrz} & C_{\theta zrz} & C_{rzrz} & C_{rzr\theta}\\ C_{rrr\theta} & C_{\theta\theta r\theta} & C_{zzr\theta} & C_{\theta zr\theta} & C_{rzr\theta} & C_{r\theta r\theta}\end{bmatrix},\quad \boldsymbol{\varepsilon}=\begin{bmatrix}\varepsilon_{rr}\\ \varepsilon_{\theta\theta}\\ \varepsilon_{zz}\\ 2\varepsilon_{z\theta}\\ 2\varepsilon_{rz}\\ 2\varepsilon_{r\theta}\end{bmatrix},\quad \boldsymbol{\alpha}=\begin{bmatrix}\alpha_{rr}\\ \alpha_{\theta\theta}\\ \alpha_{zz}\\ 2\alpha_{z\theta}\\ 2\alpha_{rz}\\ 2\alpha_{r\theta}\end{bmatrix}.\tag{3}$$

$\boldsymbol{C}$ is the fourth order stiffness tensor, $\boldsymbol{\alpha}$ is the second order tensor of thermal coefficients, ϑ is the temperature and ϑ_{ref} is a reference temperature. Ignoring inertia forces, the equations of equilibrium read

$$\frac{\partial\sigma_{rr}}{\partial r}+\frac{1}{r}\frac{\partial\sigma_{r\theta}}{\partial\theta}+\frac{\partial\sigma_{rz}}{\partial z}+\frac{\sigma_{rr}-\sigma_{\theta\theta}}{r}+f_r=0,\tag{4}$$

$$\frac{\partial\sigma_{r\theta}}{\partial r}+\frac{1}{r}\frac{\partial\sigma_{\theta\theta}}{\partial\theta}+\frac{\partial\sigma_{z\theta}}{\partial z}+2\frac{\sigma_{r\theta}}{r}+f_\theta=0,\tag{5}$$

$$\frac{\partial\sigma_{zr}}{\partial r}+\frac{1}{r}\frac{\partial\sigma_{z\theta}}{\partial\theta}+\frac{\partial\sigma_{zz}}{\partial z}+\frac{\sigma_{zr}}{r}+f_z=0.\tag{6}$$

Finally, the energy equation for steady state heat flow, ignoring the elastic mechanical energy, is written

$$-\left(\frac{\partial q_r}{\partial r}+\frac{1}{r}\frac{\partial q_\theta}{\partial\theta}+\frac{\partial q_z}{\partial z}+\frac{q_r}{r}\right)=-Q\tag{7}$$

with

$$\begin{aligned}
q_r&=-\left(\kappa_{rr}\frac{\partial\vartheta}{\partial r}+\kappa_{r\theta}\frac{1}{r}\frac{\partial\vartheta}{\partial\theta}+\kappa_{rz}\frac{\partial\vartheta}{\partial z}\right),\\
q_\theta&=-\left(\kappa_{r\theta}\frac{\partial\vartheta}{\partial r}+\kappa_{\theta\theta}\frac{1}{r}\frac{\partial\vartheta}{\partial\theta}+\kappa_{\theta z}\frac{\partial\vartheta}{\partial z}\right),\\
q_z&=-\left(\kappa_{rz}\frac{\partial\vartheta}{\partial r}+\kappa_{\theta z}\frac{1}{r}\frac{\partial\vartheta}{\partial\theta}+\kappa_{zz}\frac{\partial\vartheta}{\partial z}\right),
\end{aligned}\tag{8}$$

where $\boldsymbol{\kappa}$ is the second order thermal conductivity tensor. We note that the tensors $\boldsymbol{C}$, $\boldsymbol{\alpha}$ and $\boldsymbol{\kappa}$ are all positive definite. The term Q, which refers to radiation, the body forces $\boldsymbol{f}$ and the reference temperature ϑ_{ref} will be assumed without micro-fluctuations, being only functions of the macro-position.

As Fig. 1 shows, exact cylindrical periodicity in fiber composites implies fibers of different section, which leads to the same volume fraction and one unit cell to be solved. However, such microstructural geometry has no practical interest. A realistic situation needs the same fiber section. As we will see in Section 3.4, the proposed methodology can be used for such composites through the approximate locally periodic homogenization.

[1] We note that the Voigt notation is a way to rewrite a fourth order symmetric tensor A_{ijkl} in a 6×6 matrix form $A_{\zeta\eta}$, by applying the substitutions: $11\to1$, $22\to2$, $33\to3$, $23\to4$, $31\to5$, $12\to6$. In cylindrical coordinates we apply the substitutions: $rr\to1$, $\theta\theta\to2$, $zz\to3$, $\theta z\to4$, $rz\to5$, $r\theta\to6$.

3. Asymptotic expansion homogenization in cylindrical coordinates

The effective thermomechanical properties of the composite will be obtained using the asymptotic expansion homogenization method. This method has been used successfully for thermoelastic problems in the case of structures with periodicity in Cartesian coordinate system (Ene, 1983). In this approach two scales are considered, the macroscale and the microscale with characteristic length δ. In cylindrical coordinates we have the macro-coordinates $\boldsymbol{x}=(r,\theta,z)$ and the micro-coordinates $\boldsymbol{y}=(\frac{r}{\delta},\frac{\theta}{\delta},\frac{z}{\delta})\rightarrow(\bar{r},\bar{\theta},\bar{z})$. For clarity and simplification, we use indicial notation, where the classical (1,2,3) notation is substituted by the (r,θ,z) of cylindrical coordinates. Additionally, we introduce the operators $\mathcal{L}_i$ for the macroscale and $\bar{\mathcal{L}}_i$, $i=r,\theta,z$, for the microscale, where

$$\mathcal{L}_r=\frac{\partial}{\partial r},\quad \mathcal{L}_\theta=\frac{1}{r}\frac{\partial}{\partial\theta},\quad \mathcal{L}_z=\frac{\partial}{\partial z}, \tag{9}$$

$$\bar{\mathcal{L}}_r=\frac{\partial}{\partial\bar{r}},\quad \bar{\mathcal{L}}_\theta=\frac{1}{r}\frac{\partial}{\partial\bar{\theta}},\quad \bar{\mathcal{L}}_z=\frac{\partial}{\partial\bar{z}}. \tag{10}$$

The aim of the asymptotic expansion homogenization (AEH) method is to identify the behavior of the composite material, when the size of the microstructure becomes infinitesimally small, i.e. $\delta\rightarrow 0$. In the sequel, every quantity with the superscript δ refers to the heterogeneous material. Using (9), the strain–displacement relations (1) of the material system read

$$\begin{aligned}
&\varepsilon^\delta_{rr}=\mathcal{L}_r u^\delta_r,\quad \varepsilon^\delta_{\theta\theta}=\mathcal{L}_\theta u^\delta_\theta+\frac{u^\delta_r}{r},\quad \varepsilon^\delta_{zz}=\mathcal{L}_z u^\delta_z,\\
&\varepsilon^\delta_{\theta z}=\frac{1}{2}\left(\mathcal{L}_\theta u^\delta_z+\mathcal{L}_z u^\delta_\theta\right),\quad \varepsilon^\delta_{rz}=\frac{1}{2}\left(\mathcal{L}_r u^\delta_z+\mathcal{L}_z u^\delta_r\right),\\
&\varepsilon^\delta_{r\theta}=\frac{1}{2}\left(\mathcal{L}_r u^\delta_\theta+\mathcal{L}_\theta u^\delta_r-\frac{u^\delta_\theta}{r}\right).
\end{aligned} \tag{11}$$

In what follows, the indices i, j, k, l, m, n take the values r, θ, z and when they are repeated, the Einstein summation is used. The equilibrium equations (4)–(6) are written as

$$\begin{aligned}
&\mathcal{L}_j\sigma^\delta_{rj}+\frac{\sigma^\delta_{rr}-\sigma^\delta_{\theta\theta}}{r}+f_r=0,\quad \mathcal{L}_j\sigma^\delta_{\theta j}+2\frac{\sigma^\delta_{r\theta}}{r}+f_\theta=0,\\
&\mathcal{L}_j\sigma^\delta_{zj}+\frac{\sigma^\delta_{rz}}{r}+f_z=0.
\end{aligned} \tag{12}$$

Also, the Hooke's law (2) is written

$$\sigma^\delta_{ij}=C^\delta_{ijkl}[\varepsilon^\delta_{kl}-\alpha^\delta_{kl}(\vartheta^\delta-\vartheta_{ref})], \tag{13}$$

where the stiffness components C^δ_{ijkl} and the thermal expansion coefficient components α^δ_{ij} are generally spatially dependent. We assume that they depend on the micro-coordinates $\bar{r},\bar{\theta}$ and $\bar{z}$. Finally, the energy equation (7) reads

$$\mathcal{L}_i q^\delta_i+\frac{q^\delta_r}{r}=Q,\quad q^\delta_k=-\kappa^\delta_{kj}\mathcal{L}_j\vartheta^\delta,\quad k=r,\theta,z. \tag{14}$$

According to the AEH method, the displacements and temperature are written in a series expansion form

$$\begin{aligned}
&u^\delta_i=u^{(0)}_i(\boldsymbol{x},\boldsymbol{y})+\delta u^{(1)}_i(\boldsymbol{x},\boldsymbol{y})+\delta^2u^{(2)}_i(\boldsymbol{x},\boldsymbol{y})+\cdots,\\
&\vartheta^\delta=\vartheta^{(0)}(\boldsymbol{x},\boldsymbol{y})+\delta\vartheta^{(1)}(\boldsymbol{x},\boldsymbol{y})+\delta^2\vartheta^{(2)}(\boldsymbol{x},\boldsymbol{y})+\cdots
\end{aligned} \tag{15}$$

where $u^{(M)}_i$ and $\vartheta^{(M)}$, $M=0,1,2,\ldots$, are the expanded terms of the displacements and the temperature respectively, assumed to be periodic functions with respect to the micro-coordinates. The derivatives

$$\partial/\partial r,\quad \partial/\partial\theta,\quad \partial/\partial z$$

are substituted by

$$\partial/\partial r+\frac{1}{\delta}\partial/\partial\bar{r},\quad \partial/\partial\theta+\frac{1}{\delta}\partial/\partial\bar{\theta},\quad \partial/\partial z+\frac{1}{\delta}\partial/\partial\bar{z},$$

respectively. This leads to substitute $\mathcal{L}_i$ by $\mathcal{L}_i+\frac{1}{\delta}\bar{\mathcal{L}}_i$, $i=r,\theta,z$.

3.1. Thermal part – energy equation

The heat flux terms q_i are written in expanded form

$$q^\delta_i=\frac{1}{\delta}q^{(-1)}_i+q^{(0)}_i+\delta q^{(1)}_i+\cdots, \tag{16}$$

where

$$q^{(-1)}_i=-\kappa_{ij}\bar{\mathcal{L}}_j\vartheta^{(0)}, \tag{17}$$

$$q^{(M)}_i=-\kappa_{ij}\mathcal{L}_j\vartheta^{(M)}-\kappa_{ij}\bar{\mathcal{L}}_j\vartheta^{(M+1)},\quad M=0,1,2,\ldots \tag{18}$$

The expansion term "-1" is used for convenience in order to keep similar notation for the macroscale (index 0) and the microscale (index 1) problem with the current literature (Sanchez-Palencia, 1978; Ene, 1983). It arises from the assumption that the temperature term $\vartheta^{(0)}$ generally depends on both the macroscale and the microscale. As it is shown, eventually $\vartheta^{(0)}$ is not a function of micro-coordinates and the "-1" term is zero, not causing any issues to the homogenization problem. Similar approach is also followed for the mechanical part of the problem.

Using the expanded form of the heat fluxes (16), the energy equation takes the form

$$\begin{aligned}
&\frac{1}{\delta^2}\bar{\mathcal{L}}_i q^{(-1)}_i+\frac{1}{\delta}\left(\mathcal{L}_i q^{(-1)}_i+\bar{\mathcal{L}}_i q^{(0)}_i+\frac{q^{(-1)}_r}{r}\right)+\mathcal{L}_i q^{(0)}_i+\bar{\mathcal{L}}_i q^{(1)}_i\\
&+\frac{q^{(0)}_r}{r}-Q+\delta\ldots=0.
\end{aligned} \tag{19}$$

According to the classical procedure of the AEH method, the δ^{-2} terms must be zero. This leads to

$$\bar{\mathcal{L}}_i\kappa_{ij}\bar{\mathcal{L}}_j\vartheta^{(0)}=0. \tag{20}$$

By virtue of the periodicity of the $\vartheta^{(0)}$, the linearity in the microscale of Eq. (20), and the positive definite character of κ_{ij}, the term $\vartheta^{(0)}$ is independent of $\boldsymbol{y}$. So $q^{(-1)}_i=0$. The micro-equations are defined from the δ^{-1} terms

$$\bar{\mathcal{L}}_i q^{(0)}_i=0, \tag{21}$$

or

$$\bar{\mathcal{L}}_i(\kappa_{ij})\mathcal{L}_j\vartheta^{(0)}+\bar{\mathcal{L}}_i\left(\kappa_{ij}\bar{\mathcal{L}}_j\vartheta^{(1)}\right)=0. \tag{22}$$

In Eq. (22), $\vartheta^{(0)}$ depends only on the macro-coordinates. Assuming $\vartheta^{(0)}$ known, we can write

$$\vartheta^{(1)}=W^m\mathcal{L}_m\vartheta^{(0)}, \tag{23}$$

where W^m must satisfy the auxiliary partial differential equation problem

$$\bar{\mathcal{L}}_i\left(\kappa_{im}+\kappa_{ij}\bar{\mathcal{L}}_jW^m\right)=0,\quad W^m \text{ periodic in } (\bar{r},\bar{\theta},\bar{z}). \tag{24}$$

The final form of the micro-equations (24) allows to solve for the unknown functions W^m. Also, we need to impose the necessary continuity conditions

$$[\![W^m]\!]=0,\quad [\![\left(\kappa_{im}+\kappa_{ij}\bar{\mathcal{L}}_jW^m\right)n_i]\!]=0, \tag{25}$$

where n_i is the unit normal vector to the surface of discontinuity. The heat fluxes $q^{(0)}_i$ then are written

$$q^{(0)}_i=-\left(\kappa_{im}+\kappa_{ij}\bar{\mathcal{L}}_jW^m\right)\mathcal{L}_m\vartheta^{(0)}. \tag{26}$$

The macro-equations can be obtained from the δ^0 terms of the equilibrium equations. When δ approaches zero, every δ periodic

function tends to its weak limit, which is equal to the volume integral of the function in the periodic unit cell divided by the volume. We introduce the volume integral symbol on the volume V of the 3-D unit cell in $(\bar{r},\bar{\theta},\bar{z})$,

$$\langle\phi\rangle = \frac{r}{V}\int_V \phi(\bar{r},\bar{\theta},\bar{z})\mathrm{d}\bar{r}\,\mathrm{d}\bar{\theta}\,\mathrm{d}\bar{z}. \tag{27}$$

By setting ω_i as the outer unit normal vector to the boundary and ∂V the boundary surface of the unit cell, we can use the Gauss theorem and the periodicity of $q_i^{(1)}$ to show that

$$\langle\bar{\mathcal{L}}_i q_i^{(1)}\rangle = \frac{r}{V}\int_{\partial V} q_i^{(1)}\omega_i\,\mathrm{d}S = 0. \tag{28}$$

The macro-equations then are obtained from the weak limit of the δ^0 terms in the energy equation

$$\mathcal{L}_i\langle q_i^{(0)}\rangle + \frac{\langle q_r^{(0)}\rangle}{r} - Q = 0, \tag{29}$$

where

$$\langle q_i^{(0)}\rangle = -\langle\kappa_{im} + \kappa_{ij}\bar{\mathcal{L}}_j W^m\rangle\mathcal{L}_m\vartheta^{(0)}. \tag{30}$$

From the last equation we identify the effective thermal conductivity $\boldsymbol{\kappa}^h$ as

$$\kappa_{im}^h = \langle\kappa_{im} + \kappa_{ij}\bar{\mathcal{L}}_j W^m\rangle, \tag{31}$$

where W^m are the solutions of Eq. (24).

3.2. Mechanical part

Using (15) and the expansion of the derivatives, the strains in (11) can be written in the form

$$\varepsilon_{ij}^{\delta} = \frac{1}{\delta}\varepsilon_{ij}^{(-1)} + \varepsilon_{ij}^{(0)} + \delta\varepsilon_{ij}^{(1)} + \cdots, \tag{32}$$

where

$$\varepsilon_{ij}^{(-1)} = \frac{1}{2}\left(\bar{\mathcal{L}}_i u_j^{(0)} + \bar{\mathcal{L}}_j u_i^{(0)}\right), \tag{33}$$

$$\varepsilon_{ij}^{(M)} = \varepsilon_{ij}^{(M)*} + \frac{1}{2}\left(\bar{\mathcal{L}}_i u_j^{(M+1)} + \bar{\mathcal{L}}_j u_i^{(M+1)}\right), \quad M = 0,1,2,\ldots \tag{34}$$

and

$$\begin{aligned}
&\varepsilon_{rr}^{(M)*} = \mathcal{L}_r u_r^{(M)}, \quad \varepsilon_{\theta\theta}^{(M)*} = \mathcal{L}_\theta u_\theta^{(M)} + \frac{u_r^{(M)}}{r}, \quad \varepsilon_{zz}^{(M)*} = \mathcal{L}_z u_z^{(M)},\\
&\varepsilon_{\theta z}^{(M)*} = \frac{1}{2}\left(\mathcal{L}_z u_\theta^{(M)} + \mathcal{L}_\theta u_z^{(M)}\right), \quad \varepsilon_{rz}^{(M)*} = \frac{1}{2}\left(\mathcal{L}_r u_z^{(M)} + \mathcal{L}_z u_r^{(M)}\right),\\
&\varepsilon_{r\theta}^{(M)*} = \frac{1}{2}\left(\mathcal{L}_\theta u_r^{(M)} + \mathcal{L}_r u_\theta^{(M)} - \frac{u_\theta^{(M)}}{r}\right).
\end{aligned} \tag{35}$$

From the Hooke's law (13) and Eq. (32) we can write the expanded form of the stresses

$$\sigma_{ij}^{\delta} = \frac{1}{\delta}\sigma_{ij}^{(-1)} + \sigma_{ij}^{(0)} + \delta\sigma_{ij}^{(1)} + \cdots, \tag{36}$$

where

$$\begin{aligned}
&\sigma_{ij}^{(-1)} = C_{ijkl}\bar{\mathcal{L}}_k u_l^{(0)},\\
&\sigma_{ij}^{(0)} = C_{ijkl}\varepsilon_{kl}^{(0)*} + C_{ijkl}\bar{\mathcal{L}}_k u_l^{(1)} - C_{ijkl}\alpha_{kl}(\vartheta^{(0)} - \vartheta_{ref}),\\
&\sigma_{ij}^{(M)} = C_{ijkl}\varepsilon_{kl}^{(M)*} + C_{ijkl}\bar{\mathcal{L}}_k u_l^{(M+1)} - C_{ijkl}\alpha_{kl}\vartheta^{(M)}, \quad M = 1,2,\ldots
\end{aligned} \tag{37}$$

An interesting observation is that the reference temperature appears only on the $\sigma_{ij}^{(0)}$ components. Using the expanded form of the stresses (36), the equilibrium equations take the form

$$\begin{aligned}
&\frac{1}{\delta^2}\bar{\mathcal{L}}_j\sigma_{rj}^{(-1)} + \frac{1}{\delta}\left(\mathcal{L}_j\sigma_{rj}^{(-1)} + \bar{\mathcal{L}}_j\sigma_{rj}^{(0)} + \frac{\sigma_{rr}^{(-1)} - \sigma_{\theta\theta}^{(-1)}}{r}\right)\\
&\quad + \mathcal{L}_j\sigma_{rj}^{(0)} + \bar{\mathcal{L}}_j\sigma_{rj}^{(1)} + \frac{\sigma_{rr}^{(0)} - \sigma_{\theta\theta}^{(0)}}{r} + f_r + \delta\ldots = 0,
\end{aligned} \tag{38}$$

$$\begin{aligned}
&\frac{1}{\delta^2}\bar{\mathcal{L}}_j\sigma_{\theta j}^{(-1)} + \frac{1}{\delta}\left(\mathcal{L}_j\sigma_{\theta j}^{(-1)} + \bar{\mathcal{L}}_j\sigma_{\theta j}^{(0)} + 2\frac{\sigma_{r\theta}^{(-1)}}{r}\right)\\
&\quad + \mathcal{L}_j\sigma_{\theta j}^{(0)} + \bar{\mathcal{L}}_j\sigma_{\theta j}^{(1)} + 2\frac{\sigma_{r\theta}^{(0)}}{r} + f_\theta + \delta\ldots = 0,
\end{aligned} \tag{39}$$

$$\begin{aligned}
&\frac{1}{\delta^2}\bar{\mathcal{L}}_j\sigma_{zj}^{(-1)} + \frac{1}{\delta}\left(\mathcal{L}_j\sigma_{zj}^{(-1)} + \bar{\mathcal{L}}_j\sigma_{zj}^{(0)} + \frac{\sigma_{rz}^{(-1)}}{x_1}\right)\\
&\quad + \mathcal{L}_j\sigma_{zj}^{(0)} + \bar{\mathcal{L}}_j\sigma_{zj}^{(1)} + \frac{\sigma_{rz}^{(0)}}{x_1} + f_z + \delta\ldots = 0.
\end{aligned} \tag{40}$$

According to the classical procedure of the AEH method, the δ^{-2} terms must be zero. This leads to

$$\bar{\mathcal{L}}_j C_{ijkl}\bar{\mathcal{L}}_k u_l^{(0)} = 0, \quad i = r,\theta,z. \tag{41}$$

By virtue of the periodicity of the $u_i^{(0)}$, the linearity in the microscale of the Eq. (41), and the positive definite character of C_{ijkl}, the terms $u_i^{(0)}$ are independent of $\boldsymbol{y}$. So $\sigma_{ij}^{(-1)} = 0$. The micro-equations are defined from the δ^{-1} terms

$$\bar{\mathcal{L}}_j\sigma_{ij}^{(0)} = 0, \quad i = r,\theta,z, \tag{42}$$

which, using Eq. $(37)_2$, can be written as

$$\bar{\mathcal{L}}_j\left(C_{ijkl}\right)\varepsilon_{kl}^{(0)*} - \bar{\mathcal{L}}_j\left(C_{ijkl}\alpha_{kl}\right)(\vartheta^{(0)} - \vartheta_{ref}) + \bar{\mathcal{L}}_j\left(C_{ijkl}\bar{\mathcal{L}}_k u_l^{(1)}\right) = 0. \tag{43}$$

In Eq. (43), the terms $\varepsilon_{ij}^{(0)*}$ depend only on the macro-displacements $u_i^{(0)}$. Assuming $\varepsilon_{ij}^{(0)*}$ and $\vartheta^{(0)}$ known, we can write

$$u_i^{(1)} = N_i^{mn}\varepsilon_{mn}^{(0)*} - N_i^0(\vartheta^{(0)} - \vartheta_{ref}), \tag{44}$$

where N_i^{mn} and N_i^0 must satisfy the equations

$$\begin{aligned}
&\bar{\mathcal{L}}_j\left(C_{ijmn} + C_{ijkl}\bar{\mathcal{L}}_k N_l^{mn}\right) = 0, \quad \bar{\mathcal{L}}_j\left(C_{ijkl}\alpha_{kl} + C_{ijkl}\bar{\mathcal{L}}_k N_l^0\right) = 0,\\
&N_i^{mn}, N_i^0 \text{ periodic in } (\bar{r},\bar{\theta},\bar{z}).
\end{aligned} \tag{45}$$

The micro-equations (45) in their final form are solved for the unknown functions N_i^{mn}. Also, we need to impose the necessary continuity conditions

$$\begin{aligned}
&[\![N_i^{mn}]\!] = 0, \quad [\![(C_{ijmn} + C_{ijkl}\bar{\mathcal{L}}_k N_l^{mn})n_j]\!] = 0,\\
&[\![N_i^0]\!] = 0, \quad [\![\left(C_{ijkl}\alpha_{kl} + C_{ijkl}\bar{\mathcal{L}}_k N_l^0\right)n_j]\!] = 0,
\end{aligned} \tag{46}$$

where n_i is the unit normal vector to the surface of discontinuity. The stresses $\sigma_{ij}^{(0)}$ then are written

$$\sigma_{ij}^{(0)} = \left(C_{ijmn} + C_{ijkl}\bar{\mathcal{L}}_k N_l^{mn}\right)\varepsilon_{mn}^{(0)*} - \left(C_{ijkl}\alpha_{kl} + C_{ijkl}\bar{\mathcal{L}}_k N_l^0\right)(\vartheta^{(0)} - \vartheta_{ref}). \tag{47}$$

The macro-equations can be obtained from the δ^0 terms of the equilibrium equations. We can again use the Gauss theorem and the periodicity of $\sigma_{ij}^{(1)}$ to show that

$$\langle\bar{\mathcal{L}}_j\sigma_{ij}^{(1)}\rangle = \frac{r}{V}\int_{\partial V}\sigma_{ij}^{(1)}\omega_j\,\mathrm{d}S = 0. \tag{48}$$

Then, passing to the limit in the δ^0 macro-equations, we obtain the equilibrium equations

$$\mathcal{L}_j\langle\sigma_{rj}^{(0)}\rangle+\frac{\langle\sigma_{rr}^{(0)}\rangle-\langle\sigma_{\theta\theta}^{(0)}\rangle}{r}+f_r=0,\quad \mathcal{L}_j\langle\sigma_{\theta j}^{(0)}\rangle+2\frac{\langle\sigma_{r\theta}^{(0)}\rangle}{r}+f_\theta=0,$$
$$\mathcal{L}_j\langle\sigma_{zj}^{(0)}\rangle+\frac{\langle\sigma_{rz}^{(0)}\rangle}{r}+f_z=0, \tag{49}$$

where

$$\langle\sigma_{ij}^{(0)}\rangle=\langle C_{ijmn}+C_{ijkl}\bar{\mathcal{L}}_kN_l^{mn}\rangle\varepsilon_{mn}^{(0)*}-\langle C_{ijkl}\alpha_{kl}+C_{ijkl}\bar{\mathcal{L}}_kN_l^0\rangle \times(\vartheta^{(0)}-\vartheta_{ref}). \tag{50}$$

Last equation gives immediately that the effective medium has a constitutive law of the form

$$\langle\sigma_{ij}^{(0)}\rangle=C_{ijkl}^h[\varepsilon_{kl}^{(0)*}-\alpha_{kl}^h(\vartheta^{(0)}-\vartheta_{ref})], \tag{51}$$

where the homogenized tensors $\boldsymbol{C}^h$ and $\boldsymbol{\alpha}^h$ are given by

$$C_{ijmn}^h=\langle C_{ijmn}+C_{ijkl}\bar{\mathcal{L}}_kN_l^{mn}\rangle,$$
$$\alpha_{ij}^h=\{C_{ijmn}^h\}^{-1}\langle C_{mnkl}\alpha_{kl}+C_{mnkl}\bar{\mathcal{L}}_kN_l^0\rangle, \tag{52}$$

where the functions N_i^{mn} and N_i^0 are determined by solving the Eq. (45). The tensor $\{\boldsymbol{C}^h\}^{-1}$ is the inverse of the effective stiffness tensor.[2] It is important to note that one can possibly derive the homogenized equations using curvilinear periodicity cells. However, our approach provides a rigorous foundation of performing homogenization in curvilinear system.

We can also show that the knowledge of only N_i^{mn} is sufficient to compute $\boldsymbol{C}^h$ and $\boldsymbol{\alpha}^h$. Following Kalamkarov and Kolpakov (1997), Eq. (45) can be written

$$\bar{\mathcal{L}}_j(C_{ijmn}+C_{ijkl}\bar{\mathcal{L}}_kN_l^{mn})N_i^0=0, \tag{53}$$

and

$$\bar{\mathcal{L}}_j\left(C_{ijkl}\alpha_{kl}+C_{ijkl}\bar{\mathcal{L}}_kN_l^0\right)N_i^{mn}=0. \tag{54}$$

Using the volume integral and integrating by parts, we take into account the periodicity of these functions and we get

$$\langle C_{ijmn}\bar{\mathcal{L}}_jN_i^0\rangle+\langle C_{ijkl}\bar{\mathcal{L}}_kN_l^{mn}\bar{\mathcal{L}}_jN_i^0\rangle=0 \tag{55}$$

and

$$\langle C_{ijkl}\alpha_{kl}\bar{\mathcal{L}}_jN_i^{mn}\rangle+\langle C_{ijkl}\bar{\mathcal{L}}_kN_l^0\bar{\mathcal{L}}_jN_i^{mn}\rangle=0. \tag{56}$$

Due to the symmetry of the stiffness tensor, the second terms of the two last equations are equal and we get (using the minor and major symmetries of the stiffness tensor)

$$\langle C_{mnkl}\bar{\mathcal{L}}_kN_l^0\rangle=\langle C_{ijkl}\alpha_{kl}\bar{\mathcal{L}}_iN_j^{mn}\rangle. \tag{57}$$

So the effective tensors can be written

$$C_{ijmn}^h=\langle C_{ijmn}+C_{ijkl}\bar{\mathcal{L}}_kN_l^{mn}\rangle,$$
$$\alpha_{ij}^h=\{C_{ijmn}^h\}^{-1}\gamma_{mn},\quad \gamma_{mn}=\langle C_{mnkl}\alpha_{kl}+C_{klpq}\alpha_{pq}\bar{\mathcal{L}}_kN_l^{mn}\rangle. \tag{58}$$

It is important to mention that Eqs. (24) and (45) correspond to a unit cell (UC) which depends on the macro-coordinate r. This is a significant difference with classical periodic composites with microstructural periodicity in Cartesian coordinate system. A unit cell has the characteristic that, repeated by periodicity, may cover the entire structure of the composite (Suquet, 1987). In cylindrically periodic shell structures the UC has macrovariable-dependent elementary volume. We note that the proposed method is limited for cases where the macrostructure is a hollow tube, in which $r>0$.

[2] The inverse of a fourth order tensor $\boldsymbol{C}^h$ is defined as the fourth order tensor $\{\boldsymbol{C}^h\}^{-1}$, for which $C_{ijmn}\{C_{mnkl}\}^{-1}=\frac{1}{2}(\delta_{ik}\delta_{jl}+\delta_{il}\delta_{jk})$, where δ_{ij} is the Kronecker delta.

Another qualitative difference between the two coordinate systems (cylindrical – Cartesian) is that the coordinate θ measures angles and is dimensionless, while all the Cartesian coordinates describe lengths. A contribution of this paper is to show that, despite the difference between r, θ, z and x, y, z and the related cylindrical periodicity characterizing structures which are not produced by simple repetition of the same elementary volume, the unit cell in both cases can be reduced to a cube.

In many of the examples that will follow, the UC exhibits very different scales for $\bar{\theta}$, and for $\bar{r}$, $\bar{z}$. For this reason, it is convenient to substitute the $\bar{\theta}$-coordinate with the $\bar{\bar{\theta}}=r\bar{\theta}$-coordinate, where r is the macroscale radial coordinate. With this substitution we get

$$\bar{\mathcal{L}}_r=\frac{\partial}{\partial\bar{r}},\quad \bar{\mathcal{L}}_\theta=\frac{\partial}{\partial\bar{\bar{\theta}}},\quad \bar{\mathcal{L}}_z=\frac{\partial}{\partial\bar{z}}. \tag{59}$$

One of the significant aspects of this investigation is the generation of a complete set of homogenized module for macro-level response calculations. In some applications, only limited moduli are available while others are adjusted to lie within thermomechanically admissible bounds. Calculation of thermal stresses in polymeric composites with radially and circumferentially orthotropic graphite fibres (see work by Avery and Herakovich (1986)) is one such example.

3.3. Microscale response

Additionally to the effective properties, the AEH method can provide information about the thermomechanical response in microscopic level. In many cases this information is very valuable. When considering inelastic materials, for example, it is essential to know the value of the stresses in the microscopic level. In sensoring applications, disturbances in the thermal or mechanical response in microscopic level can significantly influence the macroscopic behavior of the composite.

Using the obtained effective thermomechanical properties, the macroscale equations (29), (30), (49), (51) and (35) (for $M=0$) are solved analytically or numerically and the macro-temperature $\vartheta^{(0)}$, the macro-displacements $u_i^{(0)}$ and the macro-strains $\varepsilon_{ij}^{(0)*}$ are computed. Returning to the unit cell problems (24) and (45), the micro-fluxes and the micro-stresses are obtained from Eqs. (26) and (47) respectively, while the micro-strains are obtained from the relations

$$\varepsilon_{ij}^{(0)}=\varepsilon_{ij}^{(0)*}+\frac{1}{2}\left(\bar{\mathcal{L}}_iN_j^{mn}+\bar{\mathcal{L}}_jN_i^{mn}\right)\varepsilon_{mn}^{(0)*}. \tag{60}$$

We note that the micro-fluxes provide information about temperature gradients in the microstructure, which allow the detection of possible thermal spots in the composite that can lead to local failure.

3.4. Approximate locally periodic homogenization

In most cases, exact cylindrical periodicity is of no practical interest (see, for instance, the fiber composite of Fig. 1). Composites with increasing fiber cross sections, like the case of Fig. 1, are not easily constructed today, but the rapid advances in the manufacturing capabilities across different scales allow to think that such configurations may indeed be practically realizable at some point in the not-so-distant future: graded joints have already been introduced by researches in the 1990s in the context of large-scale structural applications. A more realistic situation though (Fig. 2) requires the same fiber cross section, thus different volume fractions and an infinity of unit cells to be solved.

In the exact cylindrical periodicity case, one unit cell is solved with a fiber dimension corresponding to the average volume fraction of the composite. The result would be a homogeneous effective material. However, it is obvious that the homogenized

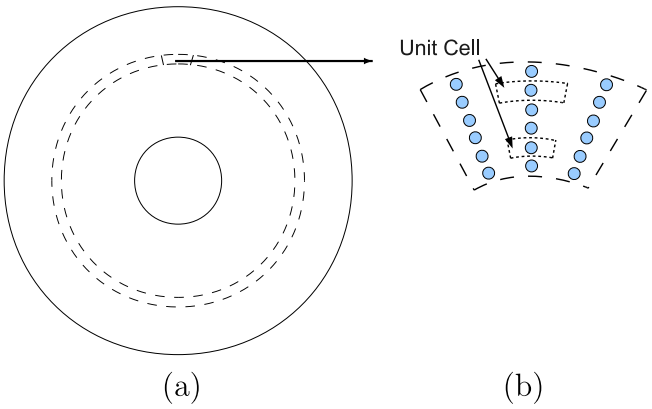

Fig. 2. Fiber composite with cylindrical geometry and a zoomed area which shows the fibers.

material of the real situation, due to the weaker zones near the outer surfaces, where the volume fraction of the fibers is smaller, can be better approximated by a graded material.

Based on this observation, we can substitute the whole volume of the composite by a sum of m small subvolumes with mean radius r_i. These subvolumes are assumed to have the same fiber volume fraction corresponding to r_i, which allows for passing to the limit and obtaining m cell problems, thus m effective zones, giving the functionally graded effective material. Fig. 3 shows how the real microstructure can be approximated to an idealized microstructure with cylindrical periodicity inside a small subvolume.

For a fiber composite, the procedure of the approximate homogenization is the following: using the experimentally defined average volume fraction of the fiber composite, one defines the number of the fibers in each subvolume, thus obtaining the fiber volume fraction of each subvolume. Then each subvolume is assumed to present exact cylindrical periodicity and its effective behavior is computed using the appropriate unit cell.

The concept of approximate locally periodic homogenization can be applied to composites with cylindrical geometry, in which the microstructure presents local periodicity.

4. Numerical examples

4.1. Multilayered cylinder

We consider a periodic structure consisting of 2 cylindrically orthotropic layers in the y_1 direction (Fig. 4). The cylindrical orthotropy is expressed by the fact that the stiffness components $C_{rr\theta z}$, C_{rrrz}, $C_{rrr\theta}$, $C_{\theta\theta\theta z}$, $C_{\theta\theta rz}$, $C_{\theta\theta r\theta}$, $C_{zz\theta z}$, C_{zzrz}, $C_{zzr\theta}$, $C_{\theta zrz}$, $C_{\theta zr\theta}$, $C_{rzr\theta}$, the coefficients of thermal expansion $\alpha_{z\theta}$, α_{rz}, $\alpha_{r\theta}$, and the thermal conductivity coefficients $\kappa_{z\theta}$, κ_{rz}, $\kappa_{r\theta}$ are zero.

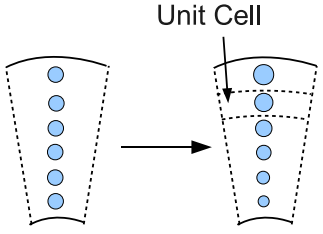

Fig. 3. Local approximation of a real fiber composite to a fiber composite with cylindrical periodicity.

Each layer has volume fraction c_w, stiffness tensor $\boldsymbol{C}^{(w)}$, coefficient of thermal expansion $\boldsymbol{\alpha}^{(w)}$ and thermal conductivity $\boldsymbol{\kappa}^{(w)}$, where $w = 1, 2$. Obviously $c_1 + c_2 = 1$.

4.1.1. Thermal part – energy equation

The solution of the micro-equations, due to the structure, must depend only on y_1. The micro-equations (24) for each material constituent w are written

$$\frac{\partial}{\partial \bar{r}}\left(\kappa_{rm}^{(w)} + \kappa_{rr}^{(w)}\frac{\partial W^{m(w)}}{\partial \bar{r}}\right) = 0 \tag{61}$$

with $m = r, \theta, z$. At the point $(\bar{r}, \bar{\bar{\theta}}, \bar{z}) = (\bar{r}_{min}, 0, 0)$ of the boundary of the unit cell we assume that all W^m are equal to a prescribed value ψ. Due to periodicity, all W^m are also equal to ψ at $(\bar{r}_{max}, 0, 0)$. Using the continuity conditions (25), Eq. (61) leads to

$$\frac{\partial W^{r(w)}}{\partial \bar{r}} = -1 + \frac{1}{\kappa_{rr}^{(w)}}\left(1 \Big/ \sum_{k=1}^{2}\frac{c_k}{\kappa_{rr}^{(k)}}\right)$$

with $w = 1, 2$, and the rest of the derivatives of W^m equal to zero.

Using the previous results and Eq. (31), the effective thermal conductivity of the composite takes the form

$$\boldsymbol{\kappa}^h = \begin{bmatrix} \kappa_{rr}^h & 0 & 0 \\ 0 & \kappa_{\theta\theta}^h & 0 \\ 0 & 0 & \kappa_{zz}^h \end{bmatrix}, \tag{62}$$

where the constituents are given explicitly as

$$\kappa_{rr}^h = 1 \Big/ \sum_{k=1}^{2}\frac{c_k}{\kappa_{rr}^{(k)}}, \quad \kappa_{\theta\theta}^h = \sum_{k=1}^{2} c_k \kappa_{\theta\theta}^{(k)}, \quad \kappa_{zz}^h = \sum_{k=1}^{2} c_k \kappa_{zz}^{(k)}. \tag{63}$$

We observe that the value ψ at the boundary does not enter the effective properties.

The micro-fluxes are given as function of the macro-temperature from the following equations:

$$q_r^{(0)(w)} = -k_{rr}^h \frac{\partial \vartheta^{(0)}}{\partial r}, \quad q_\theta^{(0)(w)} = -\frac{k_{\theta\theta}^{(w)}}{r}\frac{\partial \vartheta^{(0)}}{\partial \theta}, \quad q_z^{(0)(w)} = -k_{zz}^{(w)}\frac{\partial \vartheta^{(0)}}{\partial z}.$$

4.1.2. Mechanical part

The solution of the micro-equations, due to the geometry of the structure, depends only on y_1. Using the Voigt notation, the micro-equations $(45)_1$ for each material constituent w are written:

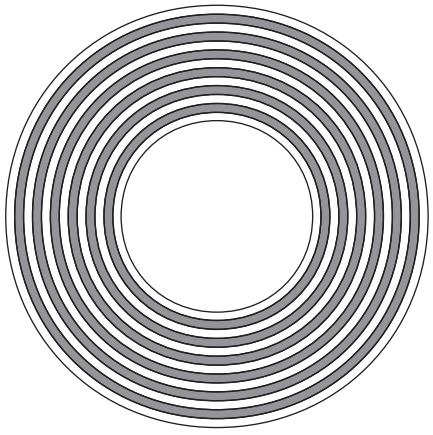

Fig. 4. Multilayered tube.

$$\frac{\partial}{\partial\bar{r}}\left(C^{(w)}_{rrmn}+C^{(w)}_{rrrr}\frac{\partial \mathrm{N}^{mn(w)}_{r}}{\partial\bar{r}}\right)=0,\quad \frac{\partial}{\partial\bar{r}}\left(C^{(w)}_{r\theta mn}+C^{(w)}_{r\theta r\theta}\frac{\partial \mathrm{N}^{mn(w)}_{\theta}}{\partial\bar{r}}\right)=0,$$
$$\frac{\partial}{\partial\bar{r}}\left(C^{(w)}_{rzmn}+C^{(w)}_{rzrz}\frac{\partial \mathrm{N}^{mn(w)}_{z}}{\partial\bar{r}}\right)=0. \tag{64}$$

with $m,n=r,\theta,z$. At the point $(\bar{r},\bar{\bar{\theta}},\bar{z})=(\bar{r}_{min},0,0)$ of the boundary of the unit cell we assume that all N^{mn} are equal to a prescribed value ψ. Due to periodicity, all N^{mn} are also equal to ψ at $(\bar{r}_{max},0,0)$. Using the continuity conditions (46)$_{1,2}$, Eq. (64) lead to

$$\frac{\partial \mathrm{N}^{mn(w)}_{r}}{\partial\bar{r}}=-\frac{C^{(w)}_{rrmn}}{C^{(w)}_{rrrr}}+\frac{1}{C^{(w)}_{rrrr}}\left(\sum_{k=1}^{2}c_k\frac{C^{(k)}_{rrmn}}{C^{(k)}_{rrrr}}\Big/\sum_{k=1}^{2}\frac{c_k}{C^{(k)}_{rrrr}}\right),\quad mn=rr,\theta\theta,zz,$$

$$\frac{\partial \mathrm{N}^{r\theta(w)}_{\theta}}{\partial\bar{r}}=-1+\frac{1}{C^{(w)}_{r\theta r\theta}}\left(1\Big/\sum_{k=1}^{2}\frac{c_k}{C^{(k)}_{r\theta r\theta}}\right),$$

$$\frac{\partial \mathrm{N}^{rz(w)}_{z}}{\partial\bar{r}}=-1+\frac{1}{C^{(w)}_{rzrz}}\left(1\Big/\sum_{k=1}^{2}\frac{c_k}{C^{(k)}_{rzrz}}\right)$$

with $w=1,2$, and the rest of the derivatives of N^{mn} equal to zero.

Using the previous results and Eq. (58)$_1$, the effective elastic stiffness of the composite takes the form

$$\boldsymbol{C}^{h}=\begin{bmatrix} C^{h}_{rrrr} & C^{h}_{rr\theta\theta} & C^{h}_{rrzz} & 0 & 0 & 0\\ C^{h}_{rr\theta\theta} & C^{h}_{\theta\theta\theta\theta} & C^{h}_{\theta\theta zz} & 0 & 0 & 0\\ C^{h}_{rrzz} & C^{h}_{\theta\theta zz} & C^{h}_{zzzz} & 0 & 0 & 0\\ 0 & 0 & 0 & C^{h}_{\theta z\theta z} & 0 & 0\\ 0 & 0 & 0 & 0 & C^{h}_{rzrz} & 0\\ 0 & 0 & 0 & 0 & 0 & C^{h}_{r\theta r\theta}\end{bmatrix}, \tag{65}$$

where the constituents are given explicitly as

$$C^{h}_{rrrr}=1\Big/\sum_{k=1}^{2}\frac{c_k}{C^{(k)}_{rrrr}},\quad C^{h}_{rr\theta\theta}=C^{h}_{rrrr}\sum_{k=1}^{2}c_k\frac{C^{(k)}_{rr\theta\theta}}{C^{(k)}_{rrrr}},$$
$$C^{h}_{rrzz}=C^{h}_{rrrr}\sum_{k=1}^{2}c_k\frac{C^{(k)}_{rrzz}}{C^{(k)}_{rrrr}},$$
$$C^{h}_{\theta\theta\theta\theta}=\sum_{k=1}^{2}c_k\left(C^{(k)}_{\theta\theta\theta\theta}-C^{(k)}_{rr\theta\theta}\frac{C^{(k)}_{rr\theta\theta}}{C^{(k)}_{rrrr}}\right)+C^{h}_{rr\theta\theta}\sum_{k=1}^{2}c_k\frac{C^{(k)}_{rr\theta\theta}}{C^{(k)}_{rrrr}},$$
$$C^{h}_{\theta\theta zz}=\sum_{k=1}^{2}c_k\left(C^{(k)}_{\theta\theta zz}-C^{(k)}_{rrzz}\frac{C^{(k)}_{rr\theta\theta}}{C^{(k)}_{rrrr}}\right)+C^{h}_{rrzz}\sum_{k=1}^{2}c_k\frac{C^{(k)}_{rr\theta\theta}}{C^{(k)}_{rrrr}},$$
$$C^{h}_{zzzz}=\sum_{k=1}^{2}c_k\left(C^{(k)}_{zzzz}-C^{(k)}_{rrzz}\frac{C^{(k)}_{rrzz}}{C^{(k)}_{rrrr}}\right)+C^{h}_{rrzz}\sum_{k=1}^{2}c_k\frac{C^{(k)}_{rrzz}}{C^{(k)}_{rrrr}},$$
$$C^{h}_{\theta z\theta z}=\sum_{k=1}^{2}c_kC^{(k)}_{\theta z\theta z},\quad C^{h}_{rzrz}=1\Big/\sum_{k=1}^{2}\frac{c_k}{C^{(k)}_{rzrz}},\quad C^{h}_{r\theta r\theta}=1\Big/\sum_{k=1}^{2}\frac{c_k}{C^{(k)}_{r\theta r\theta}}. \tag{66}$$

These results are in agreement with the results obtained in Chatzigeorgiou et al. (2008). In Chatzigeorgiou et al. (2008) several boundary value problems were solved and the effective stiffness tensor was partially computed. In the present work we obtain the complete form of the effective stiffness tensor. For the coefficients of thermal expansion, Eq. (58)$_2$ gives

$$\boldsymbol{\alpha}^{h}=\{\boldsymbol{C}^{h}\}^{-1}:\boldsymbol{\gamma}. \tag{67}$$

In the previous equation, $\boldsymbol{\gamma}$ is given by

$$\boldsymbol{\gamma}=\begin{bmatrix}\gamma_{rr} & 0 & 0\\ 0 & \gamma_{\theta\theta} & 0\\ 0 & 0 & \gamma_{zz}\end{bmatrix}, \tag{68}$$

where

$$\gamma_{rr}=C^{h}_{rrrr}\sum_{k=1}^{2}c_k\frac{C^{(k)}_{rrrr}\alpha^{(k)}_{rr}+C^{(k)}_{rr\theta\theta}\alpha^{(k)}_{\theta\theta}+C^{(k)}_{rrzz}\alpha^{(k)}_{zz}}{C^{(k)}_{rrrr}},$$
$$\gamma_{\theta\theta}=C^{h}_{rr\theta\theta}\sum_{k=1}^{2}c_k\frac{C^{(k)}_{rrrr}\alpha^{(k)}_{rr}+C^{(k)}_{rr\theta\theta}\alpha^{(k)}_{\theta\theta}+C^{(k)}_{rrzz}\alpha^{(k)}_{zz}}{C^{(k)}_{rrrr}}+\sum_{k=1}^{2}c_k\left(C^{(k)}_{\theta\theta\theta\theta}-C^{(k)}_{rr\theta\theta}\frac{C^{(k)}_{rr\theta\theta}}{C^{(k)}_{rrrr}}\right)\alpha^{(k)}_{\theta\theta}+\sum_{k=1}^{2}c_k\left(C^{(k)}_{\theta\theta zz}-C^{(k)}_{rrzz}\frac{C^{(k)}_{rr\theta\theta}}{C^{(k)}_{rrrr}}\right)\alpha^{(k)}_{zz},$$
$$\gamma_{zz}=C^{h}_{rrzz}\sum_{k=1}^{2}c_k\frac{C^{(k)}_{rrrr}\alpha^{(k)}_{rr}+C^{(k)}_{rr\theta\theta}\alpha^{(k)}_{\theta\theta}+C^{(k)}_{rrzz}\alpha^{(k)}_{zz}}{C^{(k)}_{rrrr}}+\sum_{k=1}^{2}c_k\left(C^{(k)}_{\theta\theta zz}-C^{(k)}_{rr\theta\theta}\frac{C^{(k)}_{rrzz}}{C^{(k)}_{rrrr}}\right)\alpha^{(k)}_{\theta\theta}+\sum_{k=1}^{2}c_k\left(C^{(k)}_{zzzz}-C^{(k)}_{rrzz}\frac{C^{(k)}_{rrzz}}{C^{(k)}_{rrrr}}\right)\alpha^{(k)}_{zz}. \tag{69}$$

For obtaining the mechanical response in the microscale we need to solve Eq. (58)$_2$. Using the Voigt notation for the stiffness coefficients, these equations for each material constituent are written

$$\frac{\partial}{\partial\bar{r}}\left(C^{(w)}_{rrrr}\alpha^{(w)}_{rr}+C^{(w)}_{rr\theta\theta}\alpha^{(w)}_{\theta\theta}+C^{(w)}_{rrzz}\alpha^{(w)}_{zz}+C^{(w)}_{rrrr}\frac{\partial N^{0(w)}_{r}}{\partial\bar{r}}\right)=0,$$
$$\frac{\partial}{\partial\bar{r}}\left(C^{(w)}_{r\theta r\theta}\frac{\partial N^{0(w)}_{\theta}}{\partial\bar{r}}\right)=0,\frac{\partial}{\partial\bar{r}}\left(C^{(w)}_{rzrz}\frac{\partial N^{0(w)}_{z}}{\partial\bar{r}}\right)=0. \tag{70}$$

At the point $(\bar{r},\bar{\bar{\theta}},\bar{z})=(\bar{r}_{min},0,0)$ of the boundary of the unit cell we assume that all N^{0} are equal to a prescribed value ψ. Due to periodicity, all N^{0} are also equal to ψ at $(\bar{r}_{max},0,0)$. Using the continuity conditions (46)$_{3,4}$, Eq. (70) lead to

$$\frac{\partial N^{0(w)}_{r}}{\partial\bar{r}}=\frac{\gamma_{rr}-C^{(w)}_{rrrr}\alpha^{(w)}_{rr}-C^{(w)}_{rr\theta\theta}\alpha^{(w)}_{\theta\theta}-C^{(w)}_{rrzz}\alpha^{(w)}_{zz}}{C^{(w)}_{rrrr}},$$

and the rest of the derivatives of $N^{0(w)}$ equal to zero.

The micro-stresses are given as function of the macro-temperature and the macro-strain from the following equations:

$$\sigma^{(0)(w)}_{rr}=C^{h}_{rrrr}\varepsilon^{(0)*}_{rr}+C^{h}_{rr\theta\theta}\varepsilon^{(0)*}_{\theta\theta}+C^{h}_{rrzz}\varepsilon^{(0)*}_{zz}-\gamma_{rr}(\vartheta^{(0)}-\vartheta_{ref}),$$

$$\sigma^{(0)(w)}_{\theta\theta}=\left(C^{(w)}_{rr\theta\theta}+C^{(w)}_{rr\theta\theta}\frac{\partial N^{rr(w)}_{r}}{\partial\bar{r}}\right)\varepsilon^{(0)*}_{rr}+\left(C^{(w)}_{\theta\theta\theta\theta}+C^{(w)}_{rr\theta\theta}\frac{\partial N^{\theta\theta(w)}_{r}}{\partial\bar{r}}\right)\varepsilon^{(0)*}_{\theta\theta}+\left(C^{(w)}_{\theta\theta zz}+C^{(w)}_{rr\theta\theta}\frac{\partial N^{zz(w)}_{r}}{\partial\bar{r}}\right)\varepsilon^{(0)*}_{zz}-\left(C^{(w)}_{rr\theta\theta}\alpha^{(w)}_{rr}+C^{(w)}_{\theta\theta\theta\theta}\alpha^{(w)}_{\theta\theta}+C^{(w)}_{\theta\theta zz}\alpha^{(w)}_{zz}+C^{(w)}_{rr\theta\theta}\frac{\partial N^{(0)(w)}_{r}}{\partial\bar{r}}\right)\times(\vartheta^{(0)}-\vartheta_{ref}),$$

$$\sigma^{(0)(w)}_{zz}=\left(C^{(w)}_{rrzz}+C^{(w)}_{rrzz}\frac{\partial N^{rr(w)}_{r}}{\partial\bar{r}}\right)\varepsilon^{(0)*}_{rr}+\left(C^{(w)}_{\theta\theta zz}+C^{(w)}_{rrzz}\frac{\partial N^{\theta\theta(w)}_{r}}{\partial\bar{r}}\right)\varepsilon^{(0)*}_{\theta\theta}+\left(C^{(w)}_{zzzz}+C^{(w)}_{rrzz}\frac{\partial N^{zz(w)}_{r}}{\partial\bar{r}}\right)\varepsilon^{(0)*}_{zz}-\left(C^{(w)}_{rrzz}\alpha^{(w)}_{rr}+C^{(w)}_{\theta\theta zz}\alpha^{(w)}_{\theta\theta}+C^{(w)}_{zzzz}\alpha^{(w)}_{zz}+C^{(w)}_{rrzz}\frac{\partial N^{(0)(w)}_{r}}{\partial\bar{r}}\right)\times(\vartheta^{(0)}-\vartheta_{ref}),$$

$$\sigma^{(0)(w)}_{\theta z}=C^{(w)}_{\theta z\theta z}\varepsilon^{(0)*}_{\theta z},$$

$$\sigma^{(0)(w)}_{rz}=\left(C^{(w)}_{rzrz}+C^{(w)}_{rzrz}\frac{\partial N^{rz(w)}_{z}}{\partial\bar{r}}\right)\varepsilon^{(0)*}_{rz},$$

Table 1
Thermomechanical properties of multilayered tube constituents.

Property	Steel	Aluminum
Young modulus (GPa)	206.742	72.041
Poisson ratio	0.3	0.35
Thermal expansion coefficient (1/K)	12.265E−6	23.201E−6
Thermal conductivity (W/(m K))	65.106	207.498

Table 2
Thermomechanical effective properties of multilayered tube.

E_{rr} (GPa)	$E_{\theta\theta}$ (GPa)	α_{rr} (K^{-1})	$\alpha_{\theta\theta}$ (K^{-1})	κ_{rr} (W/m K)	$\kappa_{\theta\theta}$ (W/m K)
118.717	139.567	20.736E−6	15.249E−6	99.113	136.302

Table 3
Thermomechanical properties of FRP constituents.

Property	E-glass	Epoxy
Young modulus (GPa)	72.4	3
Poisson ratio	0.16	0.3
Thermal expansion coefficient (1/K)	5.4E−5	1E−4
Thermal conductivity (W/(m K))	0.05	3.3

$$\sigma_{r\theta}^{(0)(w)} = \left(C_{r\theta r\theta}^{(w)} + C_{r\theta r\theta}^{(w)} \frac{\partial N_{\theta}^{r\theta(w)}}{\partial \bar{r}} \right) \varepsilon_{r\theta}^{(0)*}.$$

Considering a specific numerical example, we assume a multilayered tube, consisting of steel and aluminum alloy. Their properties are presented in Table 1 (Popovich and Fedai, 1997). We assume the same volume fractions for the two materials.

The effective mechanical and thermal properties of the composite tube are shown in Table 2. As it can be seen from the results, the angular Young modulus and angular thermal conductivity are higher than the radial Young modulus and radial thermal conductivity respectively. On the contrary, the coefficient of thermal expansion is higher in the radial direction.

4.2. Unidirectional fiber-reinforced polymer tube

In this subsection we examine the effective behavior of fiber reinforced polymer (FRP) composites, consisting of E-glass fibers in an epoxy resin. FRP composites with hollow cylinder structure can be used to protect cylindrical concrete columns. Usually, two or three layers of FRP composites cover a single column. Each layer has thickness close to 1 mm. The E-glass fibers have diameter between 5–20 μm (Triantafillou, 2010. See also Bakis et al., 2002). The large number of fibers in the FRP composite, even in the thickness direction, allow the use of homogenization techniques. The homogenization is accomplished with the finite element method, using the COMSOL Multiphysics software.

We assume a unidirectional FRP composite, with the fibers parallel to the axial direction of the tube. The FRP has E-glass fiber volume fraction equal to 25%. Both the epoxy and the E-glass fibers are assumed isotropic. The thermomechanical properties of the epoxy resin and the E-glass fibers are shown in Table 3. We study two cases of fiber arrangement, the cylindrical and the tetragonal (Fig. 5).

The tetragonal arrangement violates the periodicity only at the boundaries of the tube. Since the fibers are very small compared to the size of the matrix, we can approximately neglect this boundary layer, and use the classical homogenization method for the tetragonal arrangement (Kalamkarov and Kolpakov, 1997). In this example this arrangement is used for validation of the numerical solution provided by the COMSOL Multiphysics software. The obtained effective properties of the tetragonal arrangement are compared with analytical micromechanics methods provided in the literature.

For the cylindrical arrangement, we assume that the volume fraction remains the same through the radius. In order to achieve that, we need to have more fibers at larger radii. This creates a type of "discontinuity" of fibers in the radial direction (Fig. 5b). It is important to mention that this problem is not the same with the case presented in Fig. 1. In Fig. 1 the unit cells present the same volume fraction through the increase of the fiber radius. In the present case, the unit cells preserve the constant volume fraction by having more fibers through the thickness of the tube. It is an idealized situation which allows us to apply the homogenization method with exact microstructural periodicity. However, A more realistic case would require the application of approximate locally periodic homogenization, as it is explained at Section 3.4.

The unit cells used in both the tetragonal and the cylindrical arrangements are shown in Fig. 6. As it can be seen, both are represented with square shape for the matrix and cylinder shape for the fiber. The difference is that the tetragonal arrangement is solved in the $(\frac{x}{\delta}, \frac{y}{\delta})$ space, while the cylindrical arrangement is solved in the $(\frac{r}{\delta}, r^* \frac{\theta}{\delta})$ space. The cylindrical UC depends on the

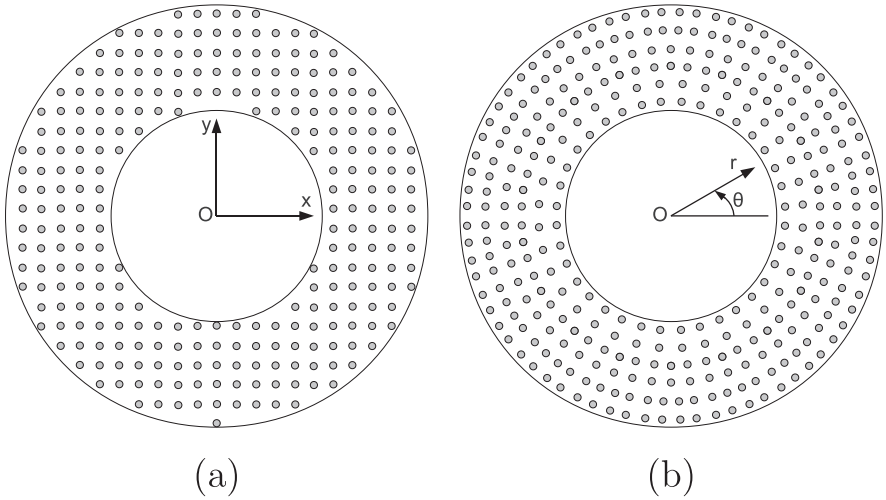

Fig. 5. Schematic of cross section of FRP composite with (a) tetragonally periodic structure and (b) cylindrically periodic structure.

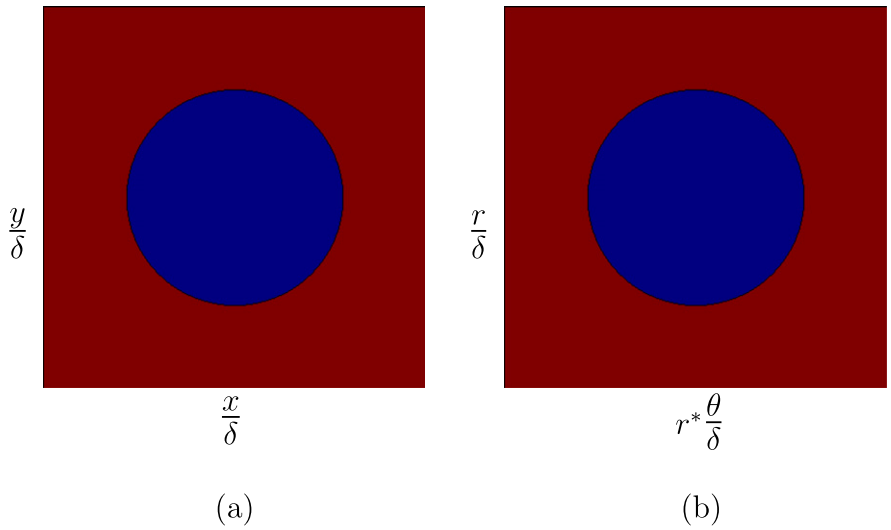

Fig. 6. Unit cell of unidirectional FRP composite for (a) tetragonally and (b) cylindrically periodic structure. The r^* denotes the macroscale radial coordinate.

Table 4
Effective properties of FRP composite with tetragonally periodic structure in Cartesian coordinates.

	AEH	Micromechanics
Mechanical properties (GPa)		
Stiffness tensor component		
$C^x_{11} = C^x_{22}$	5.9225	5.789
C^x_{33}	21.4374	21.4367
C^x_{12}	2.2411	2.373
$C^x_{13} = C^x_{23}$	2.0914	2.0912
$C^x_{44} = C^x_{55}$	1.8525	1.8516
C^x_{66}	1.6194	1.708
Thermal expansion (1/K)		
Thermal expansion coefficient component		
$\alpha^x_{11} = \alpha^x_{22}$	9.37E−5	9.75E−5
α^x_{33}	5.94E−5	5.91E−5
Thermal conductivity (W/(m K))		
Thermal conductivity component		
$\kappa^x_{11} = \kappa^x_{22}$	2.0105	2.0105
κ^x_{33}	2.4875	2.4875

Table 5
Effective properties of FRP composite with cylindrically periodic structure in Cartesian coordinates.

	AEH
Mechanical properties (GPa)	
Stiffness tensor component	
$C^x_{11} = C^x_{22}$	$5.9225 - 0.4426\frac{2x^2y^2}{(x^2+y^2)^2}$
C^x_{33}	21.4374
C^x_{12}	$2.2411 + 0.4426\frac{2x^2y^2}{(x^2+y^2)^2}$
$C^x_{13} = C^x_{23}$	2.0914
$C^x_{44} = C^x_{55}$	1.8525
C^x_{66}	$1.6194 + 0.4426\frac{2x^2y^2}{(x^2+y^2)^2}$
$C^x_{16} = -C^x_{26}$	$0.4426xy\frac{x^2-y^2}{(x^2+y^2)^2}$
Thermal expansion (1/K)	
Thermal expansion coefficient component	
$\alpha^x_{11} = \alpha^x_{22}$	9.37E−5
α^x_{33}	5.94E−5
Thermal conductivity (W/(m K))	
Thermal conductivity component	
$\kappa^x_{11} = \kappa^x_{22}$	2.0105
κ^x_{33}	2.4875

macro-coordinate r^*, which changes slowly. Since, though, the volume fraction of the fibers is constant, it suffices to solve the cylindrical UC for an arbitrary r^* only once. The boundary conditions are periodic displacements (u_x, u_y, u_z for the tetragonal arrangement and $u_r,\ u_\theta,\ u_z$ for the cylindrical arrangement) for the mechanical part, and periodic temperature for the thermal part.

The results for the tetragonal arrangement are summarized and compared with analytical micromechanics methods in Table 4.[3] The micromechanics methods that are used are the following: For the mechanical properties, the well established Mori–Tanaka method for fiber composites is used (Qu and Cherkaoui, 2006). The coefficients of thermal expansion are obtained using the Schapery method from the formulas

$$\alpha^x_{33} = \frac{E_f\alpha_f v + E_m\alpha_m(1-v)}{E_f v + E_m(1-v)},$$
$$\alpha^x_{11} = \alpha^x_{22} = (1+\nu_f)\alpha_f v + (1+\nu_m)\alpha_m(1-v) - \alpha^x_{33}[\nu_f v + \nu_m(1-v)], \tag{71}$$

where E is the Young modulus, α the thermal expansion coefficient, ν the Poisson ratio, v the fiber volume fraction and where the lower indices m and f denote matrix and fiber property respectively. The Schapery method was validated with experiments for polymeric matrix–glass fiber composites (Schapery, 1968). Since both Mori–Tanaka and Schapery are referred to random distribution of fibers in the matrix (which is equivalent to hexagonal fiber arrangement, Hashin and Rosen, 1964), the small difference between the results of the numerical and the analytical methods is expected. On the contrary, the transverse thermal conductivity is obtained with the Rayleigh's method

$$\kappa^x_{11} = \kappa^x_{22} = \kappa_m\left(1 - \frac{2v}{A + v - \frac{0.3058}{A}v^4}\right), \quad A = \frac{k_m + k_f}{k_m - k_f}, \tag{72}$$

which was designed for tetragonal arrangement fiber composites (Rayleigh, 1892). This is the reason for the excellent agreement between the numerical and the analytical results. The axial thermal conductivity is computed with the rule of mixtures.

For the cylindrically periodic structure, we obtain the effective stiffness tensor

[3] The upper index ^{x} in the properties denotes that the numbering refers to Cartesian coordinate system, where $(1,2,3) \to (x,y,z)$.

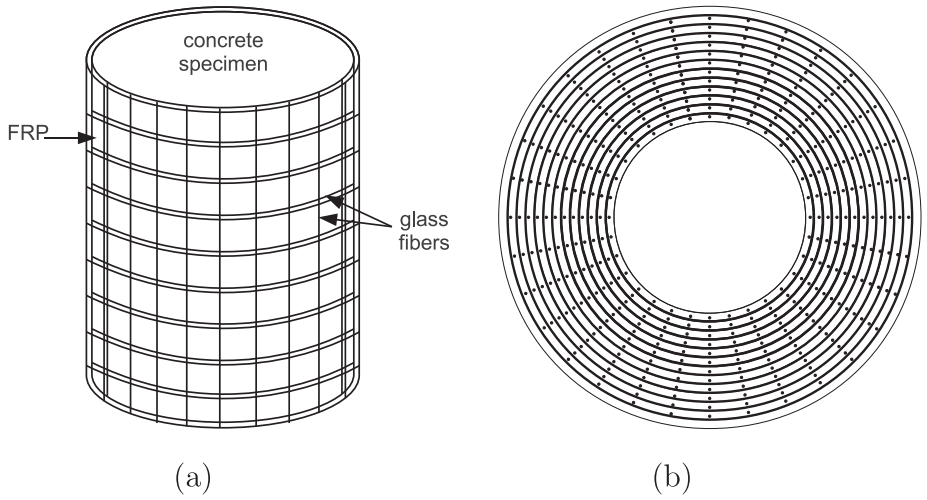

Fig. 7. (a) Concrete cylinder wrapped with FRP composite. (b) Schematic of the cross section of FRP composite with fibers in 2 directions.

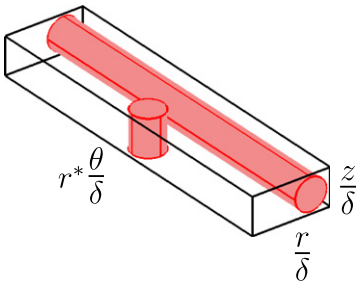

Fig. 8. Unit cell of FRP composite. The r^* denotes the macroscale radial coordinate.

Table 6
Effective properties of 2-dimensional FRP composite.

	Value (GPa)
Mechanical properties	
Stiffness tensor component	
C_{rrrr}	6.2070
$C_{\theta\theta\theta\theta}$	23.0214
C_{zzzz}	9.7505
$C_{rr\theta\theta}$	2.1366
C_{rrzz}	2.1574
$C_{\theta\theta zz}$	2.3544
$C_{\theta z\theta z}$	2.5935
C_{rzrz}	1.7829
$C_{r\theta r\theta}$	1.8334
Thermal properties	
Thermal expansion coefficient component	
α_{rr}	9.81E−5
$\alpha_{\theta\theta}$	5.96E−5
α_{zz}	7.51E−5
Thermal conductivity component	
κ_{rr}	1.3772
$\kappa_{\theta\theta}$	2.1979
κ_{zz}	2.0954

$$\boldsymbol{C}^h = \begin{bmatrix} 5.9225 & 2.2411 & 2.0914 & 0 & 0 & 0 \\ 2.2411 & 5.9225 & 2.0914 & 0 & 0 & 0 \\ 2.0914 & 2.0914 & 21.4374 & 0 & 0 & 0 \\ 0 & 0 & 0 & 1.8525 & 0 & 0 \\ 0 & 0 & 0 & 0 & 1.8525 & 0 \\ 0 & 0 & 0 & 0 & 0 & 1.6194 \end{bmatrix},$$

the effective coefficients of thermal expansion tensor

$$\boldsymbol{\alpha}^h = \begin{bmatrix} 9.37\text{E}-5 & 0 & 0 \\ 0 & 9.37\text{E}-5 & 0 \\ 0 & 0 & 5.94\text{E}-5 \end{bmatrix},$$

and the effective thermal conductivity tensor

$$\boldsymbol{\kappa}^h = \begin{bmatrix} 2.0105 & 0 & 0 \\ 0 & 2.0105 & 0 \\ 0 & 0 & 2.4875 \end{bmatrix}.$$

These properties refer to cylindrical coordinate system. In Cartesian coordinates, the stiffness tensor, the thermal conductivity tensor and the coefficient of thermal expansion tensor are computed by proper rotation from cylindrical to Cartesian coordinate system. The non-zero components are given as functions of the Cartesian coordinates x and y by the formulas given in Table 5. The obtained results are almost the same with these observed for the tetragonally periodic tube structure. The reason for this is that both the tetragonally and the cylindrically periodic structure lead to effective materials that are almost transversely isotropic with axis of symmetry parallel to the axial direction of the tube (z axis). For the thermal properties (thermal expansion and thermal conductivity), the two structures give identically the same results.

4.3. Two-directional fiber-reinforced polymer tube

This example refers to a FRP composite of tube geometry, with fibers in the axial and hoop direction. The FRP covers a cylindrical concrete specimen (Fig. 7a).

The dimensions and the properties of the example are motivated by Kshirsagar et al. (2000). We assume that the concrete specimen has a length of 20.4 cm and a diameter of 10.2 cm. The specimen's outer surface is covered with a FRP composite of thickness equal to 1.3 mm. The FRP consists of epoxy resin and E-glass fibers, whose mechanical and thermal properties are given in Table 3. The E-glass fibers are distributed in 2 directions in the epoxy. The total volume fraction of the fibers in the axial direction is taken equal to 3%, while in the hoop direction equal to 27%. The distribution of the E-glass fibers inside the epoxy is shown in the schematic cross section of Fig. 7b. In this example we assume that the E-glass fibers have a diameter equal to 8 μm. Assuming that in the thickness (or radial) direction of the FRP the fibers have the maximum density (65 axial and 65 hoop fibers), the radial distance between an axial and a hoop fiber is taken equal to 2 μm.

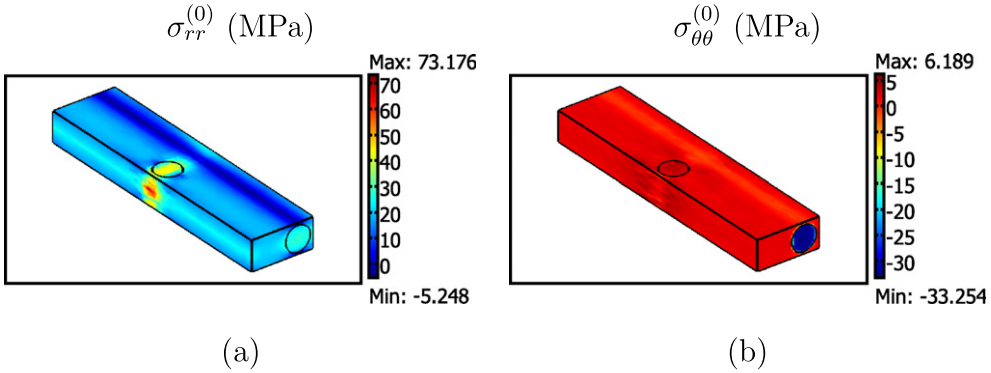

Fig. 9. Distribution of micro-stresses at a point with radial macro-strain equal to 0.005 and difference between reference and macro-temperature equal to 10 K: (a) radial stresses and (b) hoop stresses.

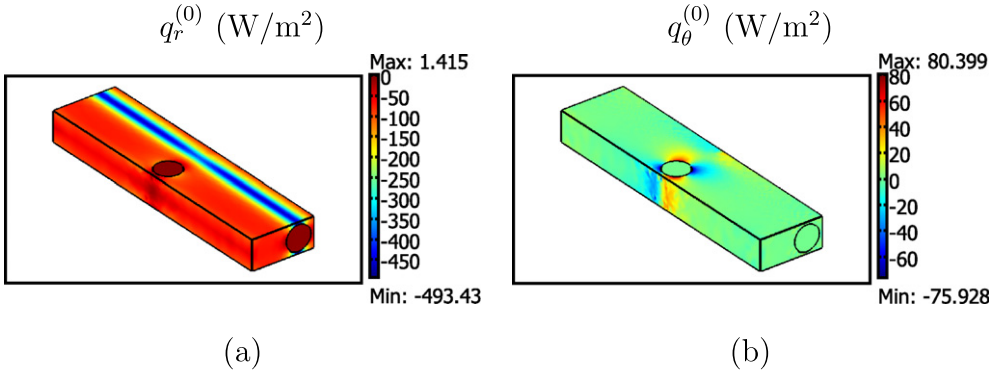

Fig. 10. Distribution of micro-fluxes at a point with macroscopic radial temperature gradient equal to 50 K/m: (a) radial heat fluxes and (b) hoop heat fluxes.

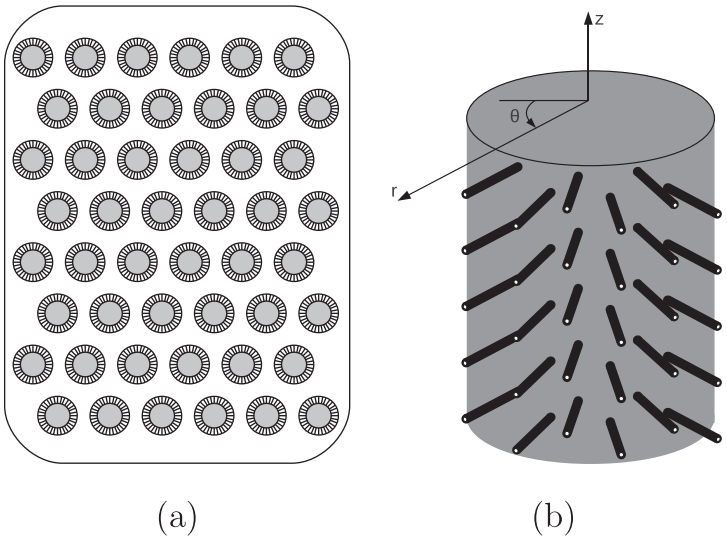

Fig. 11. Schematic of (a) fuzzy fiber composite and (b) fuzzy fiber.

Due to the uniform pattern of the axial and circumferential E-glass fibers in the FRP radial direction, the fibers volume fraction changes progressively as we move from the inner to the outer diameter of the FRP and the approximate locally periodic homogenization approach is required. Since though the radius is much larger than the thickness of the FRP, the change in fiber volume fraction is very small and can be neglected. With this approximation we need to solve only one unit cell problem, which is presented in Fig. 8. The unit cells are solved numerically with the finite element method using the COMSOL Multiphysics software. For the unit cell of Fig. 8, 31,553 triangular elements are used. The type of finite elements chosen here are the Lagrange – Quadratic.

From the numerical results (Table 6) we observe that the significant volume fraction of the hoop fibers (27%) leads to a hoop effective Young modulus of 22 GPa and hoop effective thermal

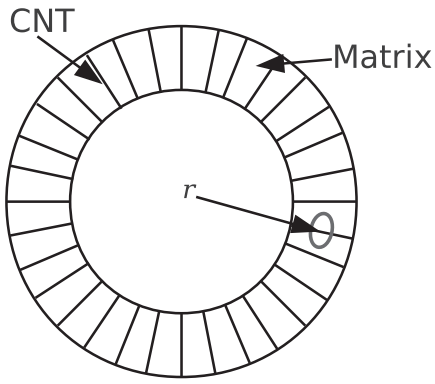

Fig. 12. Cross section of the "fuzzy fiber" interphase.

Table 7
Thermomechanical properties of layers.

EPIKOTE 862 resin	
Young modulus	3 GPa
Poisson ratio	0.3
thermal expansion coefficient	10E−5 1/K
thermal conductivity	3.3 W/(m K)
CNT	
Young modulus	1100 GPa
Poisson ratio	0.14
thermal expansion coefficient	6.5E−6 1/K
thermal conductivity	2000 W/(m K)

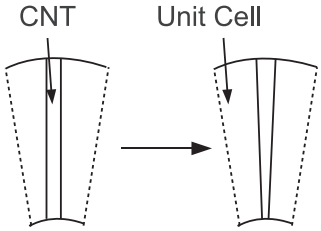

Fig. 13. Local approximation of a CNT in the composite's interphase with cylindrically periodic fiber.

expansion coefficient very close to the thermal expansion coefficient of the glass fibers.

As it is mentioned in the previous section, the proposed method allows the computation of the microscale response (stresses, strains and heat-fluxes) using macroscopic information. Considering a point in the FRP with macroscopic radial strain equal to 0.005 (the other strain components equal to zero), macroscopic difference in temperature equal to 10 K and macroscopic radial temperature gradient equal to 50 K/m (the other temperature gradients equal to zero), Figs. 9 and 10 present the micro-stresses and the micro-fluxes respectively in the radial and circumferential direction of this point.

4.4. Interphase of "fuzzy fiber" composites

The "fuzzy fiber" composite, whose interphase we want to study, is a fiber composite material system (Fig. 11a), in which a carbon fiber (CF) is coated with radially aligned carbon nanotubes (CNTs) (Fig. 11b). The "fuzzy fiber" is embedded in a matrix, which can be an epoxy. The interphase between the CF and the matrix is by itself a composite in the mesoscale level, consisting of CNTs and matrix (Fig. 12). The CNTs of the interphase are represented as hollow tubes of very large length, compared to their diameter.

The numerical examples presented in this Section are motivated by the experiments presented in Sager et al. (2009). T650 carbon fibers with diameter 5 μm are coated with radially aligned hollow carbon nanotubes of 2 μm length. The CNTs have internal radius 0.51 nm, external radius 0.85 nm. The "fuzzy fibers" are embedded in EPIKOTE 862 resin. The intermediate layer contains CNTs with average volume fraction 42.17%. The properties of the CNTs are assumed the same as the properties of the graphene (Seidel and Lagoudas, 2006). The thermomechanical properties of the epoxy resin and the CNTs are shown in Table 7.

For the computations we used the finite element program COMSOL Multiphysics. The effective properties for the interphase were obtained for hexagonal arrangement of the CNTs. Since the periodic structure of the interphase depends on the radius, we are applying the approximate locally periodic homogenization technique and several unit cells need to be solved numerically. In a subvolume, the CNT fiber cross section is represented with a fiber with the same volume and presents cylindrical periodicity (Fig. 13). Each unit cell represents a different profile of the interphase with respect to radius, and the volume fraction of the CNTs decreases as the radius increases. Fig. 14 shows several unit cells that were solved. Here the arrangement of CNTs is exactly

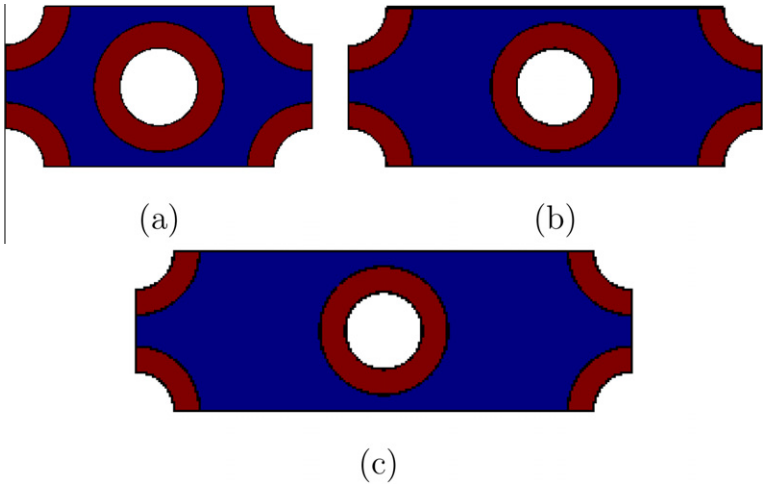

Fig. 14. Unit cell of the interphase for mesoscale r equal to (a) 2.75 μm, (b) 3.75 μm and (c) 4.5 μm. Hexagonal arrangement.

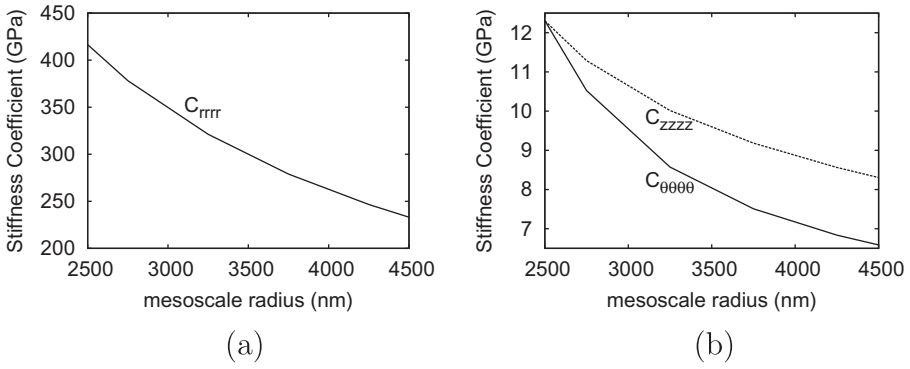

Fig. 15. Effective stiffness coefficients of the "fuzzy fiber" interphase.

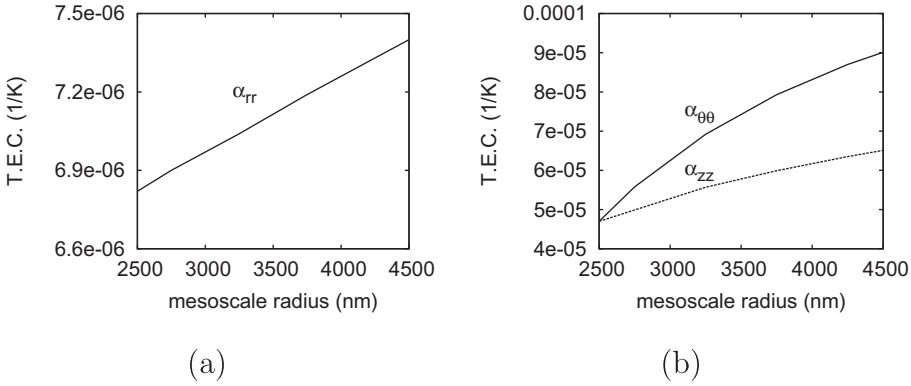

Fig. 16. Effective thermal expansion coefficients (T.E.C.) of the "fuzzy fiber" interphase.

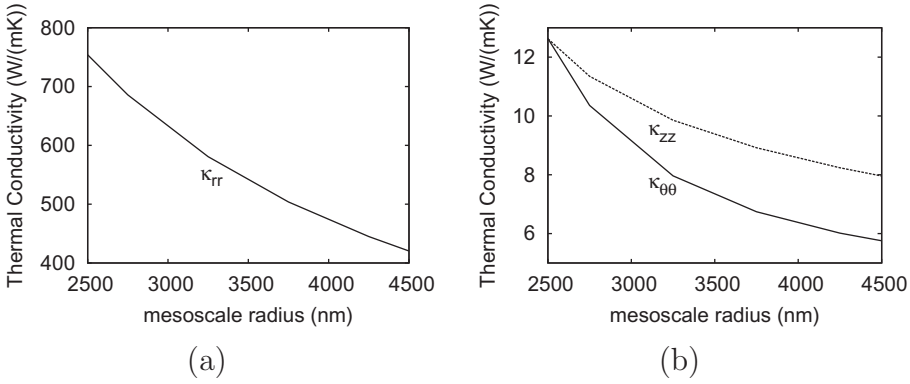

Fig. 17. Effective thermal conductivities of the "fuzzy fiber" interphase.

hexagonal only at the mesoscale radius (radius at the level of the interphase) where the carbon fiber and the interphase are connected. As we move closer to the matrix, the length of the unit cell at the y_2^* direction elongates, disturbing the hexagonal symmetry (see also Chatzigeorgiou et al., 2011).

The components of the effective stiffness coefficients C_{11}, C_{22}, C_{33}, the effective thermal coefficient and effective thermal conductivity of the "fuzzy fiber" interphase are presented in Figs. 15–17 as functions of the mesoscale radius r.

The effective interphase has orthotropic thermal behavior. The thermal expansion coefficient in the radial direction is one order of magnitude smaller than the other two coefficients (Fig. 16). On the other hand, the radial thermal conductivity is more than one order of magnitude higher than the other two conductivities (Fig. 17).

The effective thermomechanical properties of the actual "fuzzy fiber" composite can be determined using similar approach with the one discussed in Chatzigeorgiou et al. (2011) for the mechanical effective properties.

5. Conclusions

In this work we present a modified version of the asymptotic expansion homogenization method which allows for computing effective thermomechanical properties of composites with cylindrical periodicity in the microstructure. This formulation is the basis of an approximate locally periodic homogenization procedure. Additionally we are able to provide information about the micro-

scale response of the composite, computing micro-stresses, micro-strains and micro-fluxes. The proposed method is based on solving unit cells with macrovariable-dependent elementary volume and it is validated by comparing with other micromechanics techniques. Several numerical and theoretical examples of engineering interest were presented in order to check the validity and the capabilities of the proposed method. The related results could provide guidance for a way to back-out certain difficult-to-measure moduli based on limited measured data, as well as the microscale response of composites with cylindrical geometry.

Acknowledgements

The first, second and fourth authors would like to acknowledge the financial support provided by NSF, Grant No. DMR-0844082 (II-MEC project) and Grant NSF DMS 0811180. This publication is partially supported by Award No. KUS-C1-016-04, made by King Abdullah University of Science and Technology (KAUST). The first author would like to acknowledge the financial support provided by the Research Committee of Aristotle University of Thessaloniki.

References

Avery, W.B., Herakovich, C.T., 1986. Effect of fiber anisotropy on thermal stresses in fibrous composites. Journal of Applied Mechanics 53 (4), 751.

Bakhvalov, N.S., Panasenko, G.P., 1989. Homogenization: Averaged Processes in Periodic Media. Kluwer.

Bakis, C.E., Bank, L.C., Brown, V.L., Cosenza, E., Davalos, J.F., Lesko, J.J., Machida, A., Rizkalla, S.H., Triantafillou, T.C., 2002. Fiber-reinforced polymer composites for construction – state-of-the-art review. Journal of Composites for Construction 6 (2), 73–87.

Bensoussan, A., Lions, J., Papanicolaou, G., 1978. Asymptotic Methods for Periodic Structures. North Holland.

Cavalcante, M.A.A., Marques, S.P.C., Pindera, M.-J., 2007. Parametric formulation of the finite-volume theory for functionally graded materials – Part i: Analysis. Journal of Applied Mechanics 74 (5), 935–945.

Cavalcante, M.A.A., Marques, S.P.C., Pindera, M.-J., 2011. Transient finite-volume analysis of a graded cylindrical shell under thermal shock loading. Mechanics of Advanced Materials and Structures 18 (1), 53–67.

Chatzigeorgiou, G., Charalambakis, N., Murat, F., 2008. Homogenization problems of a hollow cylinder made of elastic materials with discontinuous properties. International Journal of Solids and Structures 45, 5165–5180.

Chatzigeorgiou, G., Charalambakis, N., Murat, F., 2009. Homogenization of a pressurized tube made of elastoplastic materials with discontinuous properties. International Journal of Solids and Structures 46, 3902–3913.

Chatzigeorgiou, G., Efendiev, Y., Lagoudas, D.C., 2011. Homogenization of aligned "fuzzy fiber" composites. International Journal of Solids and Structures 48 (19), 2668–2680.

Chen, T., Chung, C.-T., Lin, W.-L., 2000. A revisit of a cylindrically anisotropic tube subjected to pressuring, shearing, torsion, extension and a uniform temperature change. International Journal of Solids and Structures 37, 5143–5159.

Ene, H.I., 1983. On linear thermoelasticity of composite materials. International Journal of Engineering Science 21 (5), 443–448.

Gélébart, L., 2011. Periodic boundary conditions for the numerical homogenization of composite tubes. Comptes Rendus Mécanique 339 (1), 12–19.

Hashin, Z., Rosen, B.W., 1964. The elastic moduli of fiber-reinforced materials. Journal of Applied Mechanics 31, 223–232.

Horgan, C., Chan, A., 1999a. The pressurized hollow cylinder or disk problem for functionally graded isotropic linearly elastic materials. Journal of Elasticity 55 (1), 43–59.

Horgan, C., Chan, A., 1999b. The stress response of functionally graded isotropic linearly elastic rotating disks. Journal of Elasticity 55 (1), 219–230.

Hosseini Kordkheili, S., Naghdabadi, R., 2007. Thermoelastic analysis of a functionally graded rotating disk. Composite Structures 79, 508–516.

Iijima, S., 1991. Helical microtubules of graphitic carbon. Nature 354, 56–58.

Kalamkarov, A.L., Kolpakov, A.G., 1997. Analysis, Design and Pptimization of Composite Structures. Wiley.

Kshirsagar, S., Lopez-Anido, R.A., Gupta, R.K., 2000. Environmental aging of fiber-reinforced polymer-wrapped concrete cylinders. ACI Materials Journal 97 (6), 703–712.

Lekhnitskii, S.G., 1981. The Theory of Elasticity of an Anisotropic Body (English Translation). Mir Publishers.

Miyamoto, Y., Kaysser, W.A., Rabin, B.H., Kawasaki, A., Ford, R.G., 1999. Functionally Graded Materials: Design, Processing and Applications. Kluwer Academic Publishers.

Nie, G., Batra, R., 2010a. Exact solutions and material tailoring for functionally graded hollow circular cylinders. Journal of Elasticity 99 (2), 179–201.

Nie, G., Batra, R., 2010b. Material tailoring and analysis of functionally graded isotropic and incompressible linear elastic hollow cylinders. Composite Structures 92 (2), 265–274.

Nie, G., Batra, R., 2010c. Static deformations of functionally graded polar-orthotropic cylinders with elliptical inner and circular outer surfaces. Composites Science and Technology 70, 450–457.

Pindera, M.-J., Khatam, H., Drago, A.S., Bansal, Y., 2009. Micromechanics of spatially uniform heterogeneous media: a critical review and emerging approaches. Composites Part B: Engineering 40 (5), 349–378.

Popovich, V.S., Fedai, B.N., 1997. The axisymmetric problem of thermoelasticity of a multilayer thermosensitive tube. Journal of Mathematical Sciences 86 (2), 2605–2610.

Qu, J., Cherkaoui, M., 2006. Fundamentals of Micromechanics of Solids. John Wiley & Sons.

Rayleigh, L., 1892. On the influence of obstacles arranged in rectangular order upon the properties of a medium. Philosophy Magazine 34 (5), 481–502.

Ruhi, M., Angoshtari, A., Naghdabadi, R., 2005. Thermoelastic analysis of thick-walled finite-length cylinders of functionally graded materials. Journal of Thermal Stresses 28, 391–408.

Sager, R.J., Klein, P.J., Lagoudas, D.C., Zhang, Q., Liu, J., Dai, L., Baur, J.W., 2009. Effect of carbon nanotubes on the interfacial shear strength of T650 carbon fiber in an epoxy matrix. Composites Science and Technology 69, 898–904.

Sanchez-Palencia, E., 1978. Non-homogeneous media and vibration theory. Lecture Notes in Physics, 127. Springer-Verlag.

Schapery, R.A., 1968. Thermal expansion coefficients of composite materials based on energy principles. Journal of Composite Materials 2 (3), 380–404.

Seidel, G.D., Lagoudas, D.C., 2006. Micromechanical analysis of the effective elastic properties of carbon nanotube reinforced composites. Mechanics of Materials 38, 884–907.

Suquet, P.M., 1987. Elements of homogenization for inelastic solid mechanics. In: Sanchez-Palencia, E., Zaoui, A. (Eds.), Homogenization Techniques for Composite Materials, Lecture Notes in Physics, 272. Springer, Verlag, pp. 193–278.

Tarn, J.-Q., 2002. Exact solutions of a piezoelectric circular tube or bar under extension, torsion, pressuring, shearing, uniform electric loading and temperature change. Proceedings of the Royal Society of London 458, 2349–2367.

Tarn, J.-Q., Wang, Y.-M., 2001. Laminated composite tubes under extension, torsion, bending, shearing and pressuring: a state space approach. International Journal of Solids and Structures 38, 9053–9075.

Triantafillou, T.C., 2010. Private communication.

Tsukrov, I., Drach, B., 2010. Elastic deformation of composite cylinders with cylindrically orthotropic layers. International Journal of Solids and Structures 47, 25–33.